Geophysical Research Letters

RESEARCH LETTER
10.1029/2019GL082691

Variability in Io's Volcanism on Timescales of Periodic Orbital Changes

Katherine de Kleer[1], Francis Nimmo[2], and Edwin Kite[3]

[1]California Institute of Technology, Pasadena, CA, USA, [2]The University of California, Santa Cruz, Santa Cruz, CA, USA, [3]The University of Chicago, Chicago, IL, USA

Key Points:
- Loki Patera, Io's most powerful volcano, exhibits variability on the same timescale as the evolution of Io's orbital eccentricity and semimajor axis
- A geophysical mechanism such as poroelastic flow could amplify the importance of long-period tidal stresses relative to diurnal stresses in driving volcanism

Supporting Information:
- Supporting Information S1
- Data Set S1

Correspondence to:
K. de Kleer,
dekleer@caltech.edu

Citation:
de Kleer, K., Nimmo, F., & Kite, E. (2019). Variability in Io's volcanism on timescales of periodic orbital changes. *Geophysical Research Letters*, *46*, 6327–6332. https://doi.org/10.1029/2019GL082691

Received 6 MAR 2019
Accepted 5 MAY 2019
Accepted article online 8 MAY 2019
Published online 24 JUN 2019

Abstract The widespread volcanism on the Jovian moon Io is powered by tidal heating, yet we lack a deep understanding of how this distinctive heating process affects the locations, timing, or intensities of Io's eruptions. We show that the quasiperiodic behavior of the volcano Loki Patera in 1987–2018 matches the timescales for the evolution of Io's eccentricity and semimajor axis (~480 and ~460 days). If this orbital forcing is driving Loki Patera's variability, a low-pass geophysical filter such as poroelastic flow, or a resonant amplification of Io's wobble, could account for the importance of these long-period orbital variations despite their small amplitudes. The peak volcanic response is predicted to roughly coincide with Io's maximum eccentricity, consistent with the observations. High-cadence observations over the next several years have the potential to conclusively discriminate between orbital versus geophysical control of Loki Patera's variability.

Plain Language Summary Tidal heating is one of the central processes that generates heat in the interiors of planets and moons and is in part responsible for the existence of subsurface oceans and geological activity on moons in the outer solar system. Under this process, the amount of heating that occurs, and the stresses in the crust, vary periodically with the periodic tidal flexing. As a result, we might expect that any geological activity powered by tidal heating, such as volcanic eruptions on Jupiter's tidally heated moon Io, would also vary periodically. Indeed, the water geysers on Saturn's moon Enceladus vary in strength over the course of Enceladus' orbit around Saturn due to tides opening and closing fissures. Io takes only 1.77 days to orbit Jupiter, but its orbit is also slowly changing in time with a period of ~480 days. We compare the variability of Io's volcanoes with the evolution of its orbit and find that the quasiperiodic behavior of Loki Patera, the most powerful volcano on Io, follows a similar pattern as the orbital changes. We explore whether this volcano could be brightening and fading in response to changes in the heating and stresses produced by tides in its interior and what implications this has for the geophysical processes in Io's interior.

1. Introduction

Io is the only object in the Solar System other than Earth that is known to currently host widespread active volcanism. Io's tidally heated interior and lack of plate tectonics result in mantle and crustal conditions that contrast sharply with those of Earth (Khurana et al., 2011), providing an opportunity to understand how global planetary properties control tectonics and volcanism. Tidal stresses on a body's interior vary periodically with orbital phase, modulated by longer-term orbital changes. On Earth, seismic activity has been associated with ocean tides (Tolstoy et al., 2002). On Saturn's tidally heated moon Enceladus, water plumes jetting out from the south pole vary in strength with Enceladus' orbital phase (Hedman et al., 2013). This latter effect has been attributed to changes in the width of south polar fissures as the tidal stresses change over the course of an orbit (Hurford et al., 2007; Kite & Rubin, 2016; Nimmo et al., 2014). Longer-period modulations on this variability have also been observed, which may arise from an 11-year cycle in Enceladus' orbital eccentricity (Ingersoll & Ewald, 2017).

An analogous correlation between Io's volcanic activity and diurnal tides has not been detected to date and has been searched for at least in the case of Loki Patera (de Kleer & de Pater, 2017). However, as with Enceladus, Io's 1.77-day orbit is also modulated on longer timescales due to interactions with other objects in the system. The highest-amplitude cycles in orbital eccentricity and semimajor axis on timescales relevant to the observations follow periods of 480–484 and 461–464 days, respectively; given the relative amplitudes of these effects, the eccentricity variations should dominate the changes in tidal energy dissipation.

Observations of activity at individual Ionian volcanoes go back more than three decades (Veeder et al., 1994). In recent years, ground-based observations have substantially increased the number and cadence of measurements of activity at individual volcanoes, enhancing the suitability of the volcanic timelines for statistical comparison with cycles in Io's orbital eccentricity. The available measurements for the volcano Loki Patera are particularly extensive. This volcano puts out 10–15% of Io's total heat flow (Veeder et al., 1994), more than any other single volcano on Io, and has exhibited episodic brightenings since it was first observed in the 1980s (de Pater et al., 2017; Rathbun et al., 2002). Rathbun et al. (2002) calculated that the brightenings were periodic with a period of 540 days, although the exact interval between successive events varied by a number of months. Since then, seven more brightening cycles have been observed, and the total number of measurements has more than doubled.

2. Methods and Results

The timeline of Loki Patera's activity over the time period from 1987 to 2018, as measured from its near-infrared brightness, is shown in Figure 1a overplotted on Io's orbital eccentricity, which is smoothed to remove short-period oscillations and highlight the 480-day periodicity. The points shown in the plot and used in the analysis are the 3.5–3.8-μm brightnesses of Loki Patera derived from ground-based and *Galileo NIMS* data sets and corrected for geometric foreshortening (Davies et al., 2012; de Kleer et al., 2019; de Kleer & de Pater, 2016; de Pater et al., 2017; Rathbun & Spencer, 2006, 2010; Rathbun et al., 2002). Io's orbital eccentricity is determined for each orbit from the minimum and maximum Io-Jupiter distance over the course of the orbit, calculated from JPL Horizons data.

Figure 1b shows the same data plotted against the phase in Io's eccentricity cycle. The brightness of Loki Patera is correlated with eccentricity phase with a Spearman R coefficient of 0.39 and a p value of 10^{-12}, indicating a moderate positive correlation with a very low probability of random occurrence.

While this correlation is suggestive, a test such as this measures significance against the null hypothesis of random data, while measurements of Loki Patera's infrared brightness are clearly not independent due to the finite duration of volcanic events. To remove bias due to temporally correlated data points, we then treat each brightening cycle as a single event and determine the timing of the event by fitting a gaussian model with a duration and peak fixed at typical values. Uncertainties on the timing are determined from the earliest and latest event timing consistent with the data. For time intervals when no observations were made for longer than a typical event duration, we also determine the range of possible timings for a potential undetected event. Models for all detected and plausible undetected events are shown on the timeline of Loki Patera's infrared brightness in Figure 2a, and the timing of each event peak is shown as a function of eccentricity phase in Figure 2b.

The bright, clearly detected events (black data points) tend to peak near 0° phase. This feature is responsible for the correlation seen in Figure 1b; no brightness above 100 GW/μm/sr is seen between phases of 90° and 270°. However, the interval between events clearly varies by up to a few months, and the events overall do not occur at any preferential phase in Io's eccentricity cycle when the anomalous and plausible undetected events are included. If Loki Patera's activity is tidally controlled, the lack of consistent event phasing relative to Io's eccentricity indicates that a crustal or geological factor must be adding stochasticity to the exact event timing. Indeed, magma propagation through the lithosphere is inherently unsteady and nonuniform, so exact repeatability of each cycle cannot be expected. A similar drift in phase is seen in deep moonquake clusters (Weber et al., 2010), which are almost certainly driven by tides (Kawamura et al., 2017; Weber et al., 2009).

Figure 3a shows the day number at which each event peaks; the best-fit slope of 454.5 days/event is somewhat shorter than the 480–484 days of the eccentricity period, although the best-fit period would be longer if fewer undetected events were assumed. The residuals from this fit are shown in Figure 3b and do not show systematic trends.

We explore best-fit periods to the data, without assuming a priori how many undetected events occurred, by creating gaussian models as described above but forcing such models to be strictly periodic and fitting for the best period. Such fits find two maxima: at 452–458 (most preferred) and 479–482 days. The most preferred

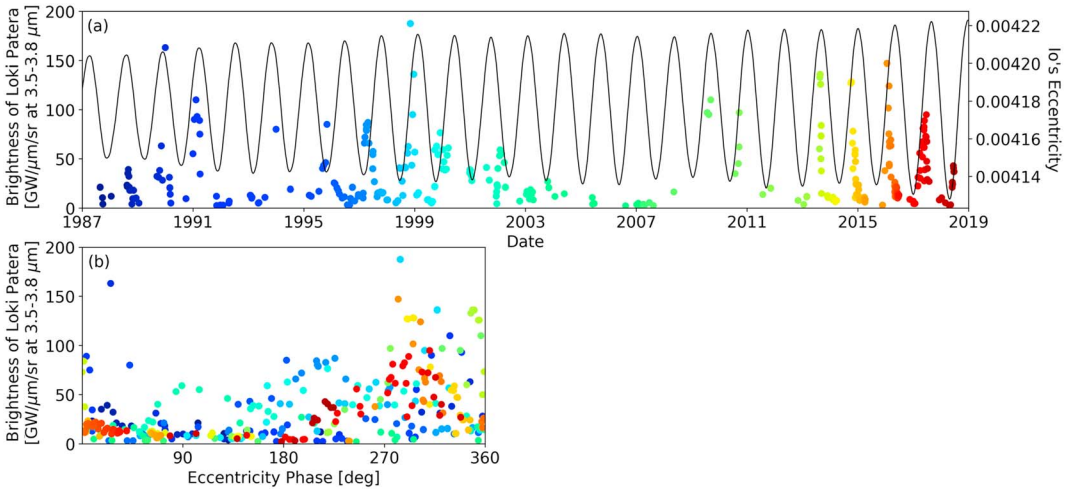

Figure 1. Loki Patera activity timeline. (a) Loki Patera's near-infrared brightness on 334 dates between 1987 and 2018. The curve is Io's eccentricity, smoothed with a 50-day window to remove short-period oscillations. (b) Loki Patera's brightness as a function of Io's eccentricity cycle; eccentricity is maximal at 0°/360° and minimal at 180°, and phase is defined for each cycle relative to the interval between maxima. Colors correspond to time and are the same as in (a) to aid in identification of groups of points belonging to single active periods. Data from Rathbun et al. (2002), Rathbun and Spencer (2006, 2010), Davies et al. (2012), de Pater et al. (2017), de Kleer and de Pater (2016), and de Kleer et al. (2019).

model (454 days) is shown with the data in Figure 4a, and the data are shown phased to this period in Figure 4b.

The irregular spacing of events results in several periods that emerge in a Fourier analysis, including both 454 and 480 days, though no peak in this range is statistically significant. The most significant period found by a periodogram is at 5,000 days, which is equal to eleven 454.5-day cycles. The upcoming few years of data will reveal whether this feature repeats in the 2019–2023 events or is a chance alignment of the stochastic component of the event timing.

These analyses show that the existing data are consistent with periodic behavior at either a 454- or 480-day period (with a stochastic timing component), both of which are remarkably close to the timescales for Io's

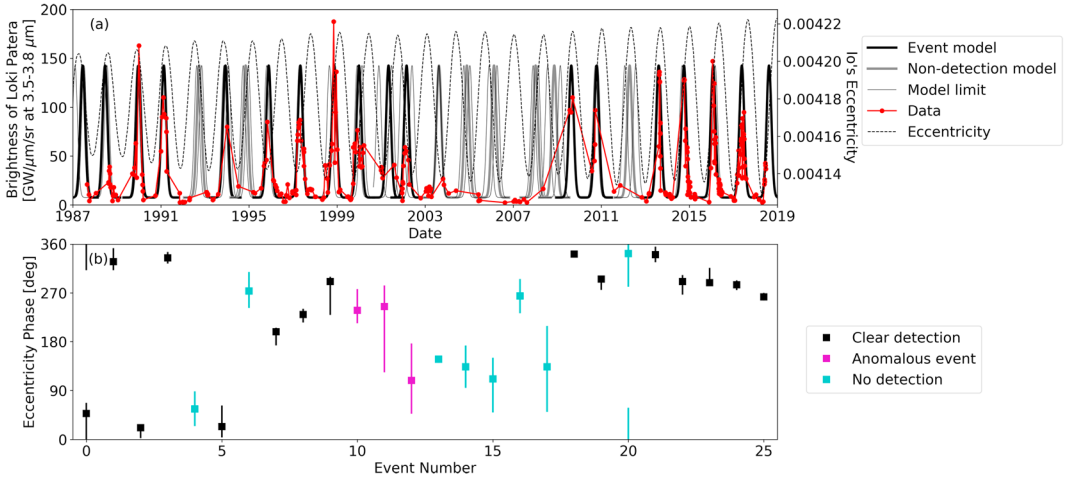

Figure 2. Best-fit event occurrences. (a) Loki Patera's timeline is shown with event models fit to the data, where the event shape is fixed and only the timing is fit for. Models are shown in black for events that are clearly detected and in gray for events that are not detected but are permitted by gaps in the data set. The thin lines bracketing the models indicate the timing uncertainties. (b) Phase of Io's eccentricity cycle at which the model events shown in (a) peak. The uncertainties correspond to the earliest and latest event timing consistent with the data. Anomalous events are those that do not follow a clear peak and decay pattern.

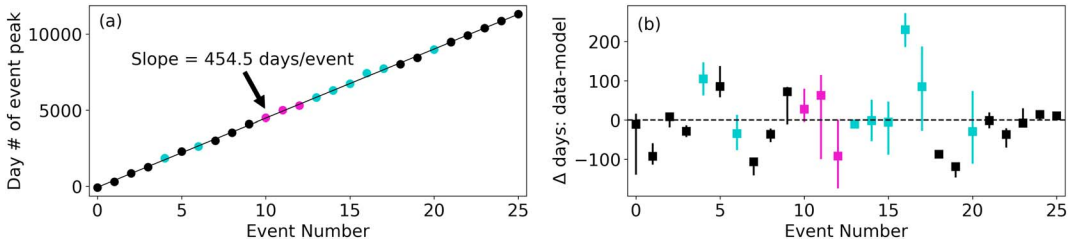

Figure 3. Event timing. (a) Timing of successive events, if all plausible undetected events occurred. The best-fit line has a slope of 454.5 days/event, somewhat shorter than the eccentricity period. (b) Event peak timing residuals from the best-fit line, showing no systematic deviations. Colors follow Figure 2b.

orbital evolution. However, the current data set cannot distinguish whether Loki Patera's brightening timescale is driven by tidal stresses or whether it is set by geophysical factors and coincidentally aligns with the orbital evolution timescales. For example, the crust-foundering model (Matson et al., 2006; Rathbun et al., 2002; Rathbun & Spencer, 2006) could be made to match this timescale by tailoring the physical properties of the lava.

The limitation in distinguishing between scenarios is the large gaps in the coverage to date. A continuation of the high cadence coverage of Loki Patera that has taken place since 2013 due to the addition of sustained monitoring with the Keck and Gemini N telescopes (de Kleer et al., 2019; de Kleer & de Pater, 2016) would have the ability to isolate a single preferred period and distinguish between orbital and geophysical controls on the eruption timescale. A projection of the 454-day cycle predicts the next events to peak near October–November 2019, January 2021, and April 2022, while if events occur at 330–360° phase in the 480-day eccentricity cycle, the next events will peak around March 2020, July 2021, and November 2022. Although the expected timing variability is up to a few months, these predicted timelines eventually diverge measurably. More generally, if any single narrow frequency emerges that characterizes the variability, then the geophysical timescale hypothesis will be increasingly disfavored and eventually eliminated because volcanic cycles have no long-term (multicycle) memory and will eventually drift in phase.

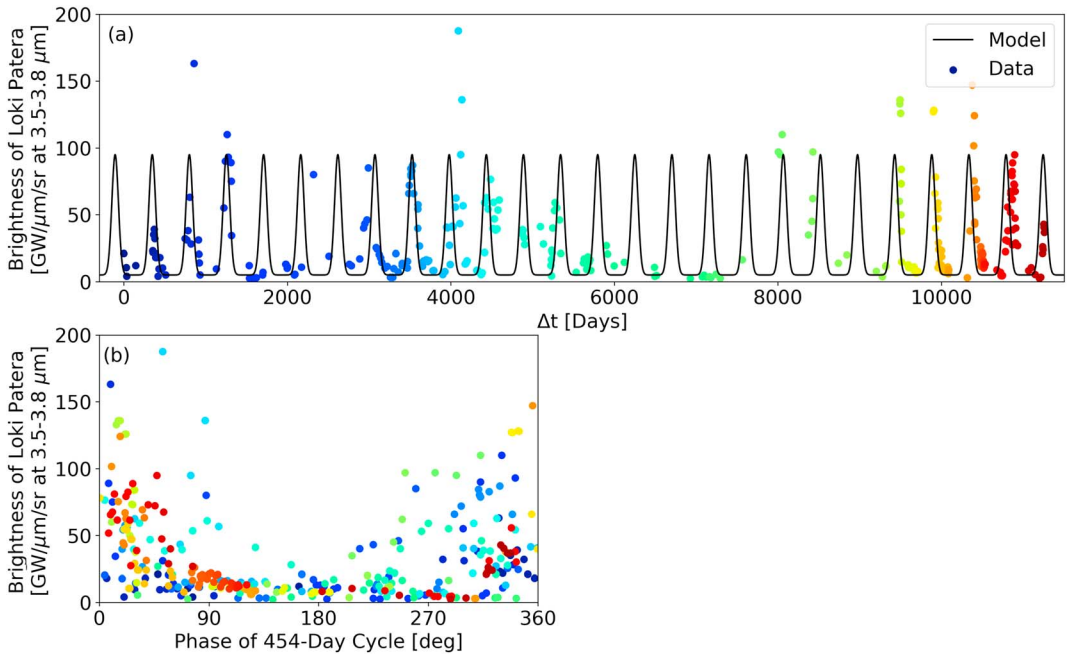

Figure 4. Best-fit period model. (a) The model is composed of strictly periodic, identical gaussian events, at the best-fit period of 454 days. (b) Data phased on the 454-day period; a phase of 0°/360° corresponds to the event peak.

3. Discussion: Geophysical Interpretation

If future data confirm that Loki Patera's activity is driven by long-period tidal effects due to Io's orbital variations, this would provide key information on how tidal forcing translates into Io's surface volcanism. In a similar manner to Enceladus, Io is subject to orbitally generated stresses from long-period librations and semi-major axis variations. Such stresses could for instance trigger dike propagation, which, if ultimately driven by slow buildup of magma chamber pressure, is more likely to occur near the most favorable phase of the stress cycle. However, unlike Enceladus, the amplitude of these long-period variations is small compared to the diurnal variations. As an example, the diurnal longitudinal libration amplitude of $2e = 0.0084$ radians is about 1,500 times the libration amplitude at the 1.3-year period (Henrard, 2005).

For these small long-period variations to be important, either the larger short-period variations are being filtered out or the long-period variations are being amplified (or both). A similar effect is seen on Earth, where fortnightly tides are as effective at triggering seismic events as diurnal tides, despite being much smaller in amplitude (van der Elst et al., 2016).

One promising filtering mechanism is poroelastic flow. The rate at which melt can be squeezed in and out of a partially molten reservoir depends on the period at which it is being forced, with longer periods leading to larger changes in melt level (see supplementary information; Doan & Brodsky, 2006; Hsieh et al., 1987; McKenzie, 1989; Nimmo et al., 2014; Smith-Konter & Pappalardo, 2008; Stolper et al., 1981; Turcotte & Schubert, 2002; Wang, 2000). Although the relevant parameters are highly uncertain, this amplification factor could be of order 10^2 when comparing 500-day with diurnal forcings. The predicted peak poroelastic response matches or slightly leads the peak eccentricity values (Figure S1 in the supporting information), consistent with the observations (Figure 1).

As a viscoelastic body, Io's tidal response will be frequency dependent. This provides one way of amplifying the effect of long-period variations. However, at least for one specific Io structural model (Bierson & Nimmo, 2016), increasing the period by a factor of 300 only increases the tidal response by a factor of 2. A more promising amplification effect arises from Io's tendency to "wobble" (and generate stresses) in response to angular momentum perturbations. The calculated wobble period, taking Io's finite rigidity into account, is 460 ± 15 days (Zharkov & Sobisevich, 2005), which overlaps with several of the long-period orbital element variations. This commensurability may be leading to resonant excitation of Io's wobble and thus enhanced long-period stresses.

The longer-baseline observations discussed above will allow us to distinguish between resonant (e.g., wobble) and low-pass filter (e.g., poroelasticity) explanations. For instance, Io experiences longitudinal librations about twice the 1.3-year amplitude at 2,060 days (Henrard, 2005). If Io is acting as a low-pass filter, then the response at 2,060 days should be a factor of a few larger than the currently observed effect. Conversely, if there is a resonance at ~460 days, we should expect to see no response from Loki Patera at a 2060 day period. A resonantly enhanced wobble at Io could in principle be directly detected using ground-based radar observations, in a similar fashion to the measurement of Europa's obliquity (Margot et al., 2013). The confirmation of either scenario from future data would represent the first evidence that tidal stresses directly influence the timing of Io's eruptions, providing new insight into the mechanisms by which tidal heating generates this satellite's extreme volcanism.

Acknowledgments
The authors are grateful to Ryan Park for providing Horizons data products, Michael E. Brown for statistics feedback, and Emily Brodsky for advice on poroelastic flow. K. d. K. is supported by the Heising-Simons Foundation through a *51 Pegasi b* postdoctoral fellowship. The authors declare no financial conflicts of interest. The data supporting the conclusions can be found in the following locations: (a) for observations prior to 2001: Rathbun et al. (2002, Figure 1), Rathbun and Spencer (2006, Figure 1), Rathbun and Spencer (2010, Figure 2); (b) for *Galileo NIMS* observations: Davies et al. (2012); and (c) for adaptive optics observations from 2001 to 2018: Data Set S1, which compiles data from de Pater et al. (2017), de Kleer and de Pater (2016), and de Kleer et al. (2019).

References

Bierson, C. J., & Nimmo, F. (2016). A test for Io's magma ocean: Modeling tidal dissipation with a partially molten mantle. *Journal of Geophysical Research: Planets*, *121*, 2211–2224. https://doi.org/10.1002/2016JE005005

Davies, A. G., Veeder, G. J., Matson, D. L., & Johnson, T. V. (2012). Io: Charting thermal emission variability with the Galileo NIMS Io Thermal Emission Database (NITED): Loki Patera. *Geophysical Research Letters: Planets*, *46*. https://doi.org/10.1029/2011GL049999

de Kleer, K., & de Pater, I. (2016). Time variability of Io's volcanic activity from near-IR adaptive optics observations on 100 nights in 2013–2015. *Icarus*, *280*, 378–404. https://doi.org/10.1016/j.icarus.2016.06.019

de Kleer, K., & de Pater, I. (2017). Io's Loki Patera: Modeling of three brightening events in 2013–2016. *Icarus*, *289*, 181–198. https://doi.org/10.1016/j.icarus.2017.01.038

de Kleer, K., de Pater, I., Molter, E. M., Banks, E., Davies, A. G., Alvarez, C., et al. (2019). Io's volcanic activity from time domain adaptive optics observations: 2013–2018. *The Astronomical Journal*, *158*, 1. https://iopscience.iop.org/article/10.3847/1538-3881/ab2380

de Pater, I., de Kleer, K., Davies, A. G., & Ádámkovics, M. (2017). Three decades of Loki Patera observations. *Icarus*, *297*, 265–281. https://doi.org/10.1016/j.icarus.2017.03.016

Doan, M.-L., & Brodsky, E. E. (2006). Tidal analysis of water level in continental boreholes: A tutorial. unpublished; https://www.pmc.ucsc.edu/~seisweb/emily_brodsky/reprints/tidal_tutorial.pdf.

Hedman, M. M., Gosmeyer, C. M., Nicholson, P. D., Sotin, C., Brown, R. H., Clark, R. N., et al. (2013). An observed correlation between plume activity and tidal stresses on Enceladus. *Nature*, *500*(7461), 182–184. https://doi.org/10.1038/nature12371

Henrard, J. (2005). The rotation of Io. *Icarus*, *178*(1), 144–153. https://doi.org/10.1016/j.icarus.2005.04.018

Hsieh, P. A., Bredehoeft, J. D., & Farr, J. M. (1987). Determination of aquifer transmissivity from earth tide analysis. *Water Resources Research*, *23*(10), 1824–1832. https://doi.org/10.1029/WR023i010p01824

Hurford, T. A., Helfenstein, P., Hoppa, G. V., Greenberg, R., & Bills, B. G. (2007). Eruptions arising from tidally controlled periodic opening of rifts on Enceladus. *Nature*, *447*(7142), 292–294. https://doi.org/10.1038/nature05821

Ingersoll, A. P., & Ewald, S. P. (2017). Decadal timescale variability of the Enceladus plumes inferred from Cassini images. *Icarus*, *282*, 260–275. https://doi.org/10.1016/j.icarus.2016.09.018

Kawamura, T., Lognonné, P., Nishikawa, Y., & Tanaka, S. (2017). Evaluation of deep moonquake source parameters: Implication for fault characteristics and thermal state. *Journal of Geophysical Research: Planets*, *122*, 1487–1504. https://doi.org/10.1002/2016JE005147

Khurana, K. K., Jia, X., Kivelson, M. G., Nimmo, F., Schubert, G., & Russell, C. T. (2011). Evidence of a global magma ocean in Io's interior. *Science*, *332*(6034), 1186–1189. https://doi.org/10.1126/science.1201425

Kite, E. S., & Rubin, A. (2016). Sustained eruptions on Enceladus explained by turbulent dissipation in tiger stripes. *Proceedings of the National Academy of Sciences*, *113*(15), 3972–3975. https://doi.org/10.1073/pnas.1520507113

Margot, J.-L., Padovan, S., Campbell, D. B., Peale, S. J., & Ghigo, F. D. (2013). Measurements of the spin states of Europa and Ganymede. *EPSC* 2013 #393

Matson, D. L., Davies, A. G., Veeder, G. J., Rathbun, J. A., Johnson, T. V., & Castillo, J. C. (2006). Io: Loki Patera as a magma sea. *Journal of Geophysical Research*, *111*, E09002. https://doi.org/10.1029/2006JE002703

McKenzie, D. (1989). Some remarks on the movement of small melt fractions in the mantle. *Earth and Planetary Science Letters*, *95*(1-2), 53–72. https://doi.org/10.1016/0012-821X(89)90167-2

Nimmo, F., Porco, F., & Mitchell, T. (2014). Tidally-modulated eruptions on Enceladus: Cassini ISS observations and models. *The Astronomical Journal*, *148*(3), 46. https://doi.org/10.1088/0004-6256/148/3/46

Rathbun, J. A., & Spencer, J. R. (2006). Loki, Io: New ground-based observations and a model describing the change from periodic overturn. *Geophysical Research Letters*, *33*, L17201. https://doi.org/10.1029/2006GL026844

Rathbun, J. A., & Spencer, J. R. (2010). Ground-based observations of time variability in multiple active volcanoes on Io. *Icarus*, *209*(2), 625–630. https://doi.org/10.1016/j.icarus.2010.05.019

Rathbun, J. A., Spencer, J. R., Davies, A. G., Howell, R. R., & Wilson, L. (2002). Loki, Io: A periodic volcano. *Geophysical Research Letters*, *29*(10), 1443. https://doi.org/10.1029/2002GL014747

Smith-Konter, B., & Pappalardo, R. T. (2008). Tidally driven stress accumulation and shear failure of Enceladus' tiger stripes. *Icarus*, *198*, 435–451. https://doi.org/10.1016/j.icarus.2008.07.005

Stolper, E., Walker, D., Hager, B. H., & Hays, J. F. (1981). Melt segregation from partially molten source regions: The importance of melt density and source region size. *Journal of Geophysical Research*, *86*(B7), 6261–6271. https://doi.org/10.1029/JB086iB07p06261

Tolstoy, M., Vernon, F. L., Orcutt, J. A., & Wyatt, F. K. (2002). Breathing of the seafloor: Tidal correlations of seismicity at Axial volcano. *Geology*, *30*(6), 503–506. https://doi.org/10.1130/0091-7613(2002)030<0503:BOTSTC>2.0.CO;2

Turcotte, D. L., & Schubert, G. (2002). *Geodynamics*. Cambridge: Cambridge University Press. https://doi.org/10.1017/CBO9780511807442

van der Elst, N. J., Delorey, A. A., Shelly, D. R., & Johnson, P. A. (2016). Fortnightly modulation of San Andreas tremor and low-frequency earthquakes. *Proceedings of the National Academy of Sciences*, *113*, 8601–8605. https://doi.org/10.1073/pnas.1524316113

Veeder, G. J., Matson, D. L., Johnson, T. V., Blaney, D. L., & Goguen, J. D. (1994). Io's heat flow from infrared radiometry: 1983-1993. *Journal of Geophysical Research*, *99*(E8), 17,095–17,162. https://doi.org/10.1029/94JE00637

Wang, H. F. (2000). *Theory of linear poroelasticity with applications to geomechanics and hydrogeology*. Princeton, NJ: Princeton University Press.

Weber, R. C., Bills, B. G., & Johnson, C. L. (2009). Constraints on deep moonquake focal mechanisms through analyses of tidal stress. *Journal of Geophysical Research*, *115*, E05001. https://doi.org/10.1029/2008JE003286

Weber, R. C., Bills, B. G., & Johnson, C. L. (2010). A simple physical model for deep moonquake occurrence times. *Physics of the Earth and Planetary Interiors*, *182*(3-4), 152–160. https://doi.org/10.1016/j.pepi.2010.07.009

Zharkov, V. N., & Sobisevich, A. L. (2005). Moments of inertia and the chandlerian period for two- and three-layer models of the Galilean satellite Io. *Astronomy Letters*, *31*(3), 205–212. https://doi.org/10.1134/1.1883352